



# Distribution of Antimicrobial Resistance and Virulence Genes within the Prophage-Associated Regions in Nosocomial Pathogens

 Kohei Kondo,<sup>a</sup>  Mitsuoki Kawano,<sup>b</sup>  Motoyuki Sugai<sup>a</sup>

<sup>a</sup>Antimicrobial Resistance Research Center, National Institute of Infectious Diseases, Higashi Murayama, Tokyo, Japan

<sup>b</sup>Department of Human Nutrition, Faculty of Contemporary Life Science, Chugokugakuen University, Kita-ku, Okayama, Japan

**ABSTRACT** Prophages are often involved in host survival strategies and contribute toward increasing the genetic diversity of the host genome. Prophages also drive horizontal propagation of various genes as vehicles. However, there are few retrospective studies contributing to the propagation of antimicrobial resistance (AMR) and virulence factor (VF) genes by prophage. We extracted the complete genome sequences of seven pathogens, including ESKAPE bacteria and *Escherichia coli* from a public database, and examined the distribution of both the AMR and VF genes in prophage-like regions. We found that the ratios of AMR and VF genes greatly varied among the seven species. More than 70% of *Enterobacter cloacae* strains had VF genes, but only 1.2% of *Klebsiella pneumoniae* strains had VF genes from prophages. AMR and VF genes are unlikely to exist together in the same prophage region except in *E. coli* and *Staphylococcus aureus*, and the distribution patterns of prophage types containing AMR genes are distinct from those of VF gene-carrying prophage types. AMR genes in the prophage were located near transposase and/or integrase. The prophage containing class 1 integrase possessed a significantly greater number of AMR genes than did prophages with no class 1 integrase. The results of this study present a comprehensive picture of AMR and VF genes present within, or close to, prophage-like elements and different prophage patterns between AMR- or VF-encoding prophage-like elements.

**IMPORTANCE** Although we believe phages play an important role in horizontal gene transfer in exchanging genetic material, we do not know the distribution of the antimicrobial resistance (AMR) and/or virulence factor (VF) genes in prophages. We collected different prophage elements from the complete genome sequences of seven species—*Enterococcus faecium*, *Staphylococcus aureus*, *Klebsiella pneumoniae*, *Acinetobacter baumannii*, *Pseudomonas aeruginosa*, *Enterobacter cloacae*, and *Escherichia coli*—and characterized the distribution of antimicrobial resistance and virulence genes located in the prophage region. While virulence genes in prophage were species specific, antimicrobial resistance genes in prophages were highly conserved in various species. An integron structure was detected within specific prophage regions such as P1-like prophage element. Maximum of 10 antimicrobial resistance genes were found in a single prophage region, suggesting that prophages act as a reservoir for antimicrobial resistance genes. The results of this study show the different characteristic structures between AMR- or VF-encoding prophages.

**KEYWORDS** antimicrobial resistance, nosocomial pathogen, prophage, prophage-like element, virulence factors

Antimicrobial resistance (AMR) is a global public health issue. In recent years, ESKAPE pathogens (*Enterococcus faecium*, *Staphylococcus aureus*, *Klebsiella pneumoniae*, *Acinetobacter baumannii*, *Pseudomonas aeruginosa*, and *Enterobacter* spp.) have

**Citation** Kondo K, Kawano M, Sugai M. 2021. Distribution of antimicrobial resistance and virulence genes within the prophage-associated regions in nosocomial pathogens. *mSphere* 6:e00452-21. <https://doi.org/10.1128/mSphere.00452-21>.

**Editor** Mariana Castanheira, JMI Laboratories

**Copyright** © 2021 Kondo et al. This is an open-access article distributed under the terms of the [Creative Commons Attribution 4.0 International license](https://creativecommons.org/licenses/by/4.0/).

Address correspondence to Kohei Kondo, [kondo-k@niid.go.jp](mailto:kondo-k@niid.go.jp).

**Received** 18 May 2021

**Accepted** 10 June 2021

**Published** 7 July 2021

become a threat since they are the leading cause of nosocomial infection and easily escape from authentic chemotherapy due to their antimicrobial-resistant phenotype, and many countries have faced difficulties in controlling these pathogens (1, 2). In Japan, *Escherichia coli* has replaced *Staphylococcus aureus* as the primary pathogen isolated from clinical samples in hospitals since 2018, and isolation of third-generation cephalosporin- or quinolone-resistant *E. coli* continues to increase in Japan (<https://janis.mhlw.go.jp>). Moreover, extended-spectrum of  $\beta$ -lactamase-producing *E. coli* is spreading worldwide (3). These ESKAPE and *E. coli* are major AMR pathogens in nosocomial settings.

A bacteriophage (phage) is a virus that infects bacteria. As soon as a phage adsorbs to the host's cell wall, the phage genome is injected into the host cell. Temperate phages follow one of the two life cycles afterward: the lysogenic cycle or the lytic cycle. In the lysogenic cycle, the phage genome is integrated into the host chromosome, and it is called a prophage. In the lytic cycle, the prophage is induced to produce progeny phages in response to chemical or physical stressors (4, 5). Temperate phages or prophages are known to drive horizontal gene transfer (HGT) through transduction, but they also play an important role in increasing the genetic diversity of the host (6–10). Furthermore, defective prophages or prophage-like elements are stable in the host genome despite deleting most of the phage genes (6) and are known to increase host survival by conferring resistance against various stresses (11–13).

Plasmid conjugation has been well established as the major means of HGT of AMR genes (14), but recent studies have shed light on the role of phages in HGT of AMR genes since they are often encoded within the genome of the phage or prophage (15, 16). Metagenomic analysis revealed that AMR genes, such as  $\beta$ -lactamase, are found in the phage genome (17–19). A clinical study reported that phages harboring AMR genes were identified in samples from patients with cystic fibrosis (20). Costa et al. reported that many prophage regions within the *A. baumannii* genome possessed several AMR and virulence factor (VF) genes using a bioinformatics approach (21). These studies have implied that phages and prophages probably transduce AMR genes more frequently than expected. However, the relationship between prophages and AMR genes has not been fully explored.

Pathogenic or VF genes in prophages have been mainly studied in *S. aureus* (22, 23), *E. coli* (24, 25), *Salmonella enterica* (26), and *Vibrio* spp. (27, 28), and their pathogenicity is associated with VFs encoded by the prophages. Other reports revealed that the expression of the Shiga toxin in *E. coli* (29) and staphylokinase (*sak*) in *S. aureus* (30) depends on prophage induction. The studies mentioned above indicate that it is important to investigate the connection between host pathogenicity and their prophage to reveal their pathogenesis. However, very little is known of the relationship between virulence and prophages in the rapidly emerging multidrug-resistant bacteria, such as ESKAPE pathogens and *E. coli*.

This study aims to understand the distribution of AMR and VF genes encoded in prophages, including the intact region, prophage-like elements, and satellite prophages (31) comprised in the bacterial genome, and to discover their specific structural genomic features beyond the genera. We focus on seven clinically important AMR pathogens, including ESKAPE pathogens and *E. coli*, and analyzed their complete genomes deposited in a database to mine the prophage structure.

## RESULTS

**Comparison of host genome size and the number of prophages and prophage-like genomic islands.** To elucidate the distribution of AMR and VF genes encoded in the prophages within the genomes of ESKAPE bacteria, we collected complete genomes and RefSeq data of seven bacterial species (169 sequences of *A. baumannii*, 27 sequences of *E. cloacae*, 324 sequences of *E. coli*, 88 sequences of *E. faecium*, 408 sequences of *K. pneumoniae*, 183 sequences of *P. aeruginosa*, and 424 sequences of *S. aureus*) from GenBank (see Data Set S1 in the supplemental material). In this study, plasmid sequences were collected from 5 *A. baumannii*, 3 *E. faecium*, 14 *K. pneumoniae*,

and 23 *S. aureus* isolates, while no plasmids were collected from *E. coli*, *E. cloacae*, and *P. aeruginosa* isolates; this was because the RefSeq plasmids of these species are not registered or are not selected. Subsequently, we detected prophages or prophage-like genomic islands in each genome using PHASTER (32). We investigated the correlation between the host genome size and the number of prophage elements present. The Pearson's correlation coefficients (*R* values) of each species were 0.57 for *A. baumannii*, 0.51 for *E. cloacae*, 0.76 for *E. coli*, 0.67 for *E. faecium*, 0.51 for *K. pneumoniae*, 0.67 for *P. aeruginosa*, and 0.63 for *S. aureus*. The *R* values for all species were >0.5, indicating that the number of prophages positively correlated with the host genome size (see Fig. S1A).

Next, we analyzed the number of prophages and prophage-like elements in each species. The number of prophages in *E. coli* was significantly higher than in other species (see Fig. S1B) ( $P < 0.001$ ): *E. coli* possessed a maximum of 24 prophages and prophage-related mobile elements (accession numbers CP027459 and CP024618), in which the prophages harboring the Shiga toxin genes *stx<sub>2A</sub>* and *stx<sub>2B</sub>* can be found.

Screening for prophage elements in plasmids yielded a few cases, as depicted in Fig. S2. Comparison of the numbers of prophages in plasmids indicated that most *K. pneumoniae* plasmids harbored at least one or more prophages or prophage-like elements, and some *S. aureus* plasmids possessed one prophage or prophage-like element. However, *A. baumannii* possessed no plasmids harboring prophage or prophage-like elements. The number of prophages harbored in *K. pneumoniae* plasmids was significantly higher than in *A. baumannii* and *S. aureus* plasmids ( $P = 4.7 \times 10^{-5}$  and  $P = 0.0011$ , respectively) (see Fig. S1). AMR genes from prophage elements were encoded in plasmids found in *K. pneumoniae* (AP018748), whereas no VF genes were detected on plasmid-harboring prophages in the accession numbers used in this experiment.

**Proportion of the number of AMR or VF genes to that of prophages in the host genome.** We screened the prophage regions to exclude genomic islands without phage-related genes (see Materials and Methods) and examined the proportion of selected prophage elements encoding either AMR or VF genes. The proportions of the strains harboring prophages encoding VF genes were relatively high in *E. cloacae*, *E. coli*, *E. faecium*, and *S. aureus* (70.4, 44.2, 38.4, and 72.3%, respectively) (Fig. 1). In contrast, no prophages with VFs were detected in *A. baumannii*. Similarly, *K. pneumoniae* and *P. aeruginosa* also showed low proportions of VFs harbored in the corresponding prophages (1.2 and 10.5%, respectively) (Fig. 1).

Prophage regions encoding AMR genes were detected in all species. The proportions were as follows: 1.8% for *A. baumannii*, 11.1% for *E. cloacae*, 8.1% for *E. coli*, 2.4% for *E. faecium*, 20.9% for *K. pneumoniae*, 12.7% for *P. aeruginosa*, and 12.6% for *S. aureus*. The proportions of the host genome that contained both AMR and VF genes in the prophages were as follows: 11.1% for *E. cloacae*, 6.2% for *E. coli*, 1.2% for *E. faecium*, 0.3% for *K. pneumoniae*, 1.1% for *P. aeruginosa*, and 9.9% for *S. aureus* (Fig. 1). Overall, the differences in proportions for each species indicated that the ratio between AMR and VF genes differed greatly depending on the species.

**Characterization of prophage types encoding either AMR or VF genes.** We investigated the phage types integrated into the genome in each species. The name of each phage type was described using the most common phage indicated by the PHASTER database. The phage types harboring AMR gene(s) are listed in Fig. 2 and aligned according to the number of phage types harboring AMR gene(s) (Fig. 2). The number of phage types harboring AMR genes was 41 (Fig. 2). Notably, the major phage types carrying AMR gene(s), i.e., Escher\_RCS47 (RCS47), Staphy\_SPbeta\_like, and Entero\_P4 phages, were present in two or more species beyond the generic barrier. The P1 phage type, which is well known as a carrier of AMR genes, was detected in *K. pneumoniae*. In addition, the RCS47 phage is closely related to the P1 temperate phage and has newly acquired the insertion sequences (ISs) IS26 and *blaSHV* (33). The RCS47 phage type was detected in *E. cloacae*, *E. coli*, and *K. pneumoniae* (Fig. 2). Our results suggest that P1-

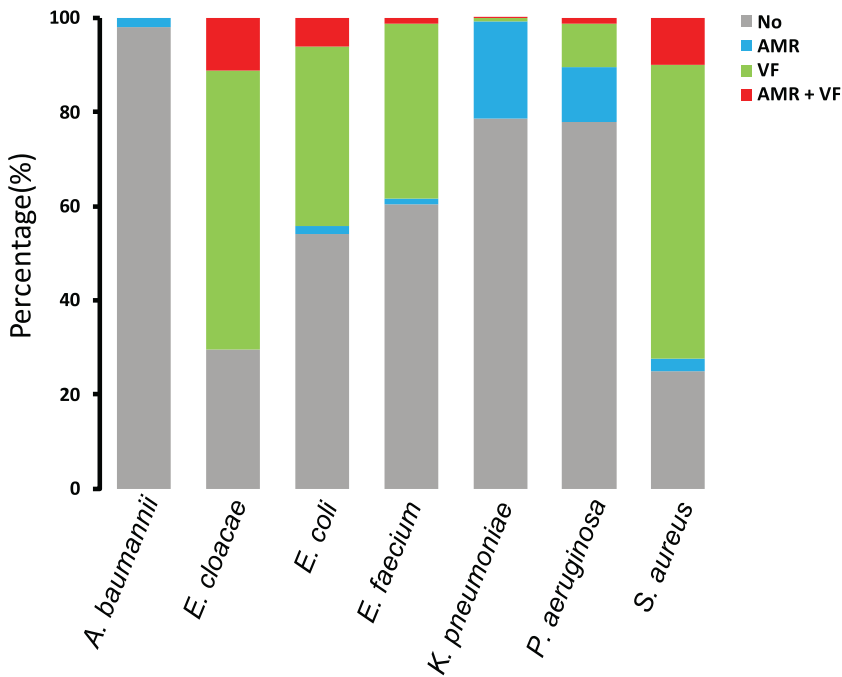


**FIG 1** Proportion of the host genomes having prophages with AMR or VF genes. A bar chart shows the genome of each species that has AMR and/or VF gene-containing prophages. Blue represents strains with AMR genes, green represents strains having VF genes, and red represents the strains having both AMR and VF genes. Gray areas indicate strains with neither AMR nor VF genes.

like phages are responsible for the transfer of AMR genes into the host genomes of bacteria from a broad range of genera.

In contrast to prophages containing AMR genes, we found that VF genes were widely distributed in a large number of phage types. There were 66 phage types; this number was 1.6-fold higher than the number of phage types harboring AMR genes. The prophage types carrying VF genes tended to be different from those harboring AMR genes, although some AMR gene-harboring prophage types were detected in VF-encoding prophages (Fig. 2). For instance, Entero\_BP\_4795 prophages, which are the most frequently detected phages carrying VF genes, were not detected in the prophages harboring AMR genes, whereas P4 phages were found to harbor AMR- and VF-encoding prophages (Fig. 2). Prophage types containing the VF genes hardly overlapped between different species. In other words, prophages containing VF genes are specific to each bacterial species. No prophages containing both AMR and VF genes are detected except in *E. coli* and *S. aureus* strains. Overall, these results indicated that AMR and VF genes rarely coexisted within the same prophage and that the distribution patterns of prophage types containing AMR genes were different from those of VF gene-carrying prophage types.

**Comparing complete genomes of prophages harboring AMR and VF genes.** We next compared the completeness of prophage-encoding regions carrying AMR and VF genes. The prophage regions were classified using criteria from PHASTER as either intact, questionable, or incomplete. As shown in Fig. 3, percentages of prophages with AMR genes were 16.6, 29.6, and 53.8% for incomplete, questionable, and intact ones, respectively. Prophages carrying VF genes were mostly intact (75.2%), which indicated that the prophage retained most of its region, whereas 16.0 and 8.8% were incomplete and questionable phages, respectively (Fig. 3A). In contrast to prophages carrying AMR genes, those carrying VF genes often encoded proteins that were crucial for the structure of the phage, such as the head, tail, and baseplate (see Data Sets S4 and S5). Evidently, all prophages encoding Shiga toxins in *E. coli* were intact and contained phage structural proteins (see Data Sets S4 and S5). Next, we compared the number of

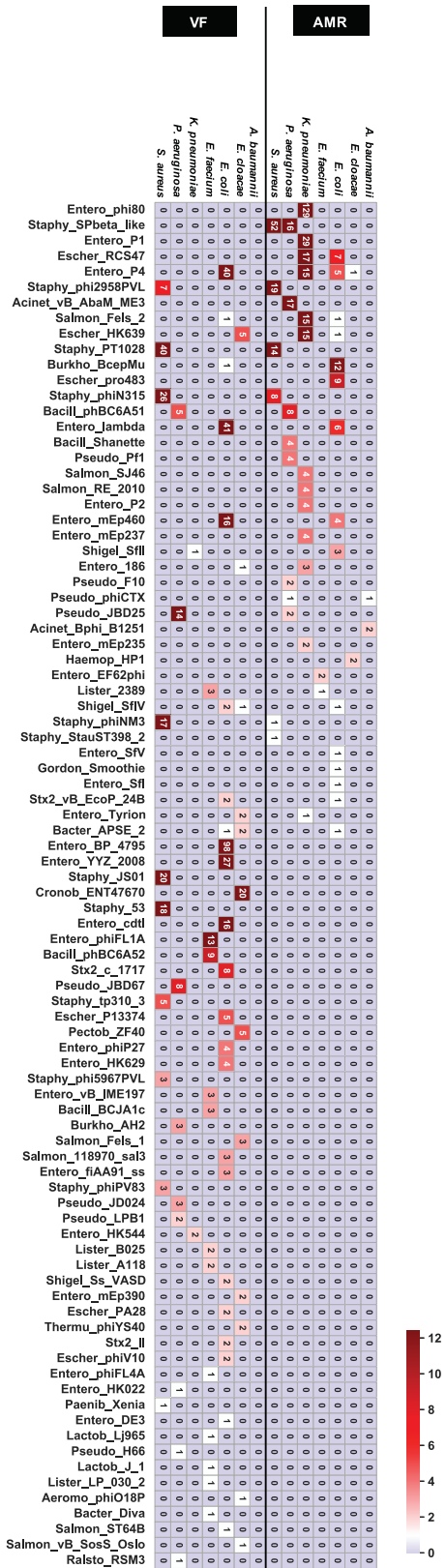


**FIG 2** Types of prophages containing AMR and VF genes. Each prophage region that possessed AMR or VF genes was classified based on the most common phage in PHASTER. A heatmap shows the abundance of prophage type in each genus. The bottom shows the prophage types described in PHASTER. The numeric character in each cell represents the number of detected phage names.

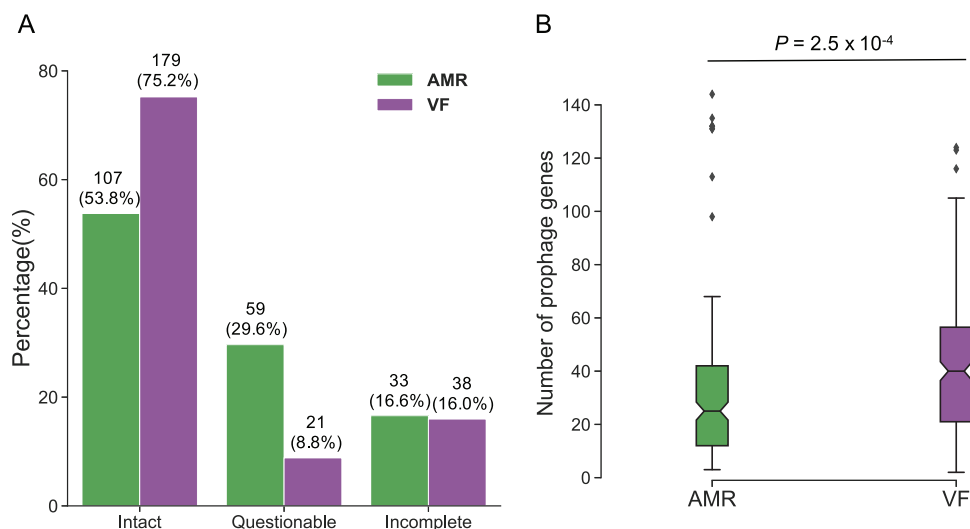


**FIG 3** Analysis of prophage completeness harboring AMR or VF genes. (A) Each prophage that had AMR or VF genes was classified as incomplete, intact, or questionable depending on the length and their completeness. The green bars show the percentage of prophages with AMR genes, the purple bars show the percentage of prophages with VF genes. The percentages regarded all AMR- or VF-encoding prophages as 100%, and the numerical character below the percentage indicates the number of samples in each classification. (B) The prophage genes were annotated using BLASTp. The genes involved in integrase, transposase, and AMR/VF genes were excluded, and the numbers of prophage genes in each region were counted. Welch's *t* test was performed, with  $P < 0.05$  considered significant.

all phage-related genes, except for transposase-, integrase-, and AMR/VF-encoding genes, in each prophage region. The number of prophage-related genes in VF-encoded prophages was more than that of AMR genes ( $P = 2.5 \times 10^{-4}$ ) (Fig. 3B). These results imply that AMR-encoding prophages are prone to be inactivated and degraded and thus are likely to become defective prophages.

**Characterization of VF genes in prophages.** To further investigate VF genes in prophage elements, VF genes for each accession number were examined using the Virulence Factors Database (VFDB) from ABRicate, and the presence of VF genes in prophages was visualized in the matrix (Fig. 4).

Prevalence of prophage-encoded VF genes was unique to each species (Fig. 4). For example, *gtrA* and *gtrB*, which encode bactoprenol-linked glucose translocase/flippase, were detected in 65.0% of *E. cloacae* strains, in one *K. pneumoniae* strain, and in one *E. coli* strain, but not in strains of other species (Fig. 4). Bacteriophage ENT47670 (accession number NC\_019927) contained *gtrA* and *gtrB*. Interestingly, intact ENT47670 prophage, which also contained structural phage proteins, was detected in the prophage region where *gtrA* and *gtrB* were harbored (see Data Sets S3 and S5). This result indicates that *gtrA* and *gtrB* of the prophage region in *E. cloacae* were acquired through the transduction of ENT47670 or ENT47670-like phages (34).

*E. faecium* strains had two specific genes in the prophage regions—*bsh* encoding a bile salt hydrolase and *clpP* encoding an ATP-dependent protease—but other species did not (Fig. 4). We mapped the prophage region harboring *bsh* and *clpP* in *E. faecium* using BRIG (35) (see Fig. S3). We found that these genes were generally located at or near the gaps in the genome and were scattered at various locations in the chromosome. It has been assumed that *bsh* genes in *E. faecium* have been transferred via HGT because the G+C content of *bsh* gene is different from the genomic G+C content of this organism (36). Our results indicate that temperate phage-mediated transduction is one of the factors responsible for the transfer of *bsh* genes in *E. faecium*.

Classification of VF genes located in prophages revealed using VFDB keywords showed that each species possesses functionally unique VF genes (see Fig. S4).

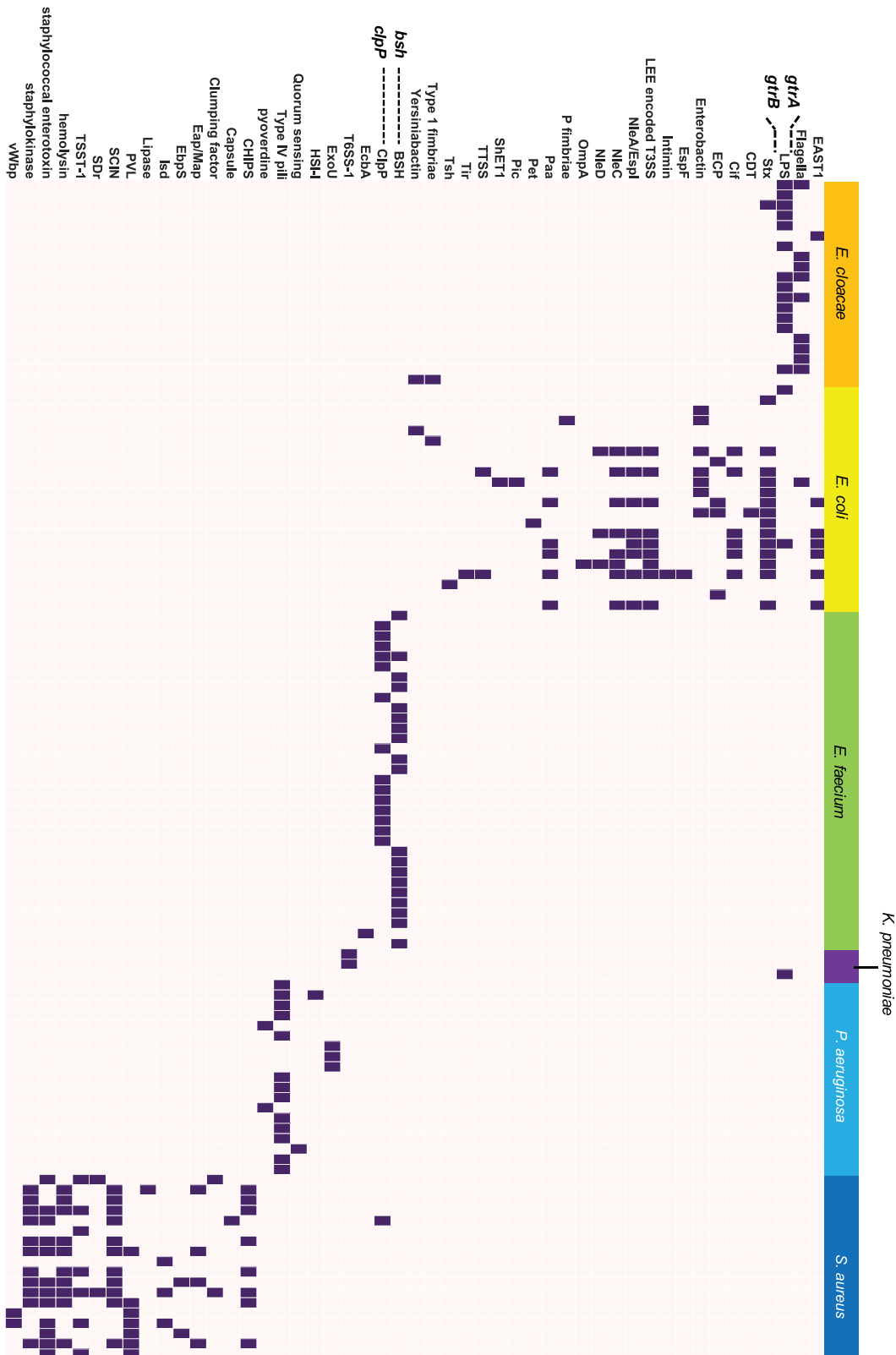


**FIG 4** Distribution of VF genes in the prophage regions. DNA sequences of the prophage regions extracted from PHASTER were examined for the presence or absence of various VF genes using the VFDB. Color in the heatmap indicates whether genes are present or not (purple square, presence, white square; absence). VF genes in *S. aureus* and *E. coli* are shown as representative strains. All VF genes harbored by prophages are listed in Data Set S3. EAST, heat-stable enterotoxin 1; CDT, cytolethal distending toxin; Cif, cyclomodulin; LEE, locus of enterocyte effacement; TTSS, type 3 secretion system; CHiPS, chemotaxis-inhibiting protein; PVL, Panton-Valentine leucocidin; SCIN, staphylococcal complement inhibitor; TSST-1, toxic shock syndrome toxin 1.

**Characterization of AMR genes encoded by or nearby prophage elements.** To investigate AMR gene distribution in the prophage elements of each strain in detail, AMR genes in the prophage region for each accession number were extracted using the ResFinder database from ABRicate and classified based on predicted substrates and mutation locations (see Materials and Methods). Aminoglycoside-modifying enzyme-associated gene(s) and  $\beta$ -lactamase are widely distributed among the seven bacterial species studied here (Fig. 5).

Apart from the genes encoding aminoglycoside-modifying enzymes and  $\beta$ -lactamase, which have been reported in various species, few species-specific AMR genes were also detected. For instance, the intact pro483 type prophage in *E. coli* (CP019256) harbored two copies of *mphA*, encoding macrolide 2'-phosphotransferase I. *vanHBX*, conferring resistance to vancomycin, was detected in only *E. faecium*, and *vanHBX* was harbored in "intact" prophages with the genes encoding some structural proteins (see Data Sets S2 and S4). These data suggested that a part of *van* family of genes in vancomycin-resistant *E. faecium* were acquired via phage transduction.

AMR gene cassettes were widely detected in various species. For instance, *K. pneumoniae* contained a cassette array of AMR genes, including *sul1*, *aadA*, and *aacA* (Fig. 5). To detect the combination or the gene cassette of AMR genes harbored by prophage elements, we classified and clustered AMR gene cassettes for each prophage type (Fig. 6). Prophage regions from 43 Entero\_phi80, 9 Entero\_P1, and 5 Escher\_HK639 harbored a set of AMR genes, including *sul1\_5*, *aac(3)\_Ib\_1* and *aadA2\_1* (Fig. 6; see also Data Set S2). Furthermore, another cassette array containing *aac(6')-aph(2'')*, *ant(6)-Ia*, *aph(3')-III*, and *ctr(C)* was detected in more than eight Staphy\_SPbeta\_like prophage regions and one Staphy\_phiN315. Since these AMR gene combinations detected on prophage regions resemble the integron cassette array, we tried to identify the integrons in these prophage regions using the INTEGRALL database. We found that specific prophage regions in *K. pneumoniae*, *E. coli*, and *P. aeruginosa* possessed class 1 integrase and AMR gene cassette arrays (see Data Set S2). Therefore, we considered these characteristic regions containing AMR genes cassette arrays as integron cassette arrays (integron-associated prophage structures). Although the structure of integron-associated prophages has been hardly reported, our results clearly reveal that specific prophage elements, including those in P1-like phages, are preserved in the genomes of ESKAPE bacteria.

Next, we wondered whether the prophage region containing integrons had a higher number of AMR genes than regions without integrons (Fig. 7). We examined the number of AMR genes in phage regions carrying integrons (Int/P, red), in those without integrons (No-Int, green), and in strains where integrons were present somewhere other than the prophage region (No-Int/P, blue).

All the phage regions carrying an integron possessed three or more AMR genes, whereas 82.7% of the phage regions without an integron possessed fewer than three AMR genes (Fig. 7A). These results indicated that the number of AMR genes were significantly higher in prophages with integrons than in other groups ( $P < 0.001$ ) (Fig. 7B).

**Structural features of prophage elements containing AMR genes.** We briefly overviewed the structural features of the prophage region and its association with AMR gene(s) by showing representative prophage sequences (Fig. 8). The prophage regions within the attachment sites (*attL* and *attR*) are shown in Fig. 8. AMR genes in intact prophage regions existed either between or near integrase and/or transposase genes (Fig. 8A and B). Furthermore, AMR genes were located at the end of the prophage region, whereas the central position in the prophage region often encoded essential phage genes, especially structural proteins. Although the intact phages Salmon\_Fels\_2 and Entero\_186 do not harbor class 1 integron integrase, phage-derived integrase was present near to AMR gene(s) (Fig. 8A and B). Next, we visualized the prophage regions from Escher\_HK639, which were described as intact or questionable phages using PHASTER (Fig. 8B). The prophage region from Escher\_HK639 contained in *K. pneumoniae* (accession number CP018816) is described as one from a questionable phage; the other three HK639 phages (shown in Fig. 8C) are intact phages, which also contain the

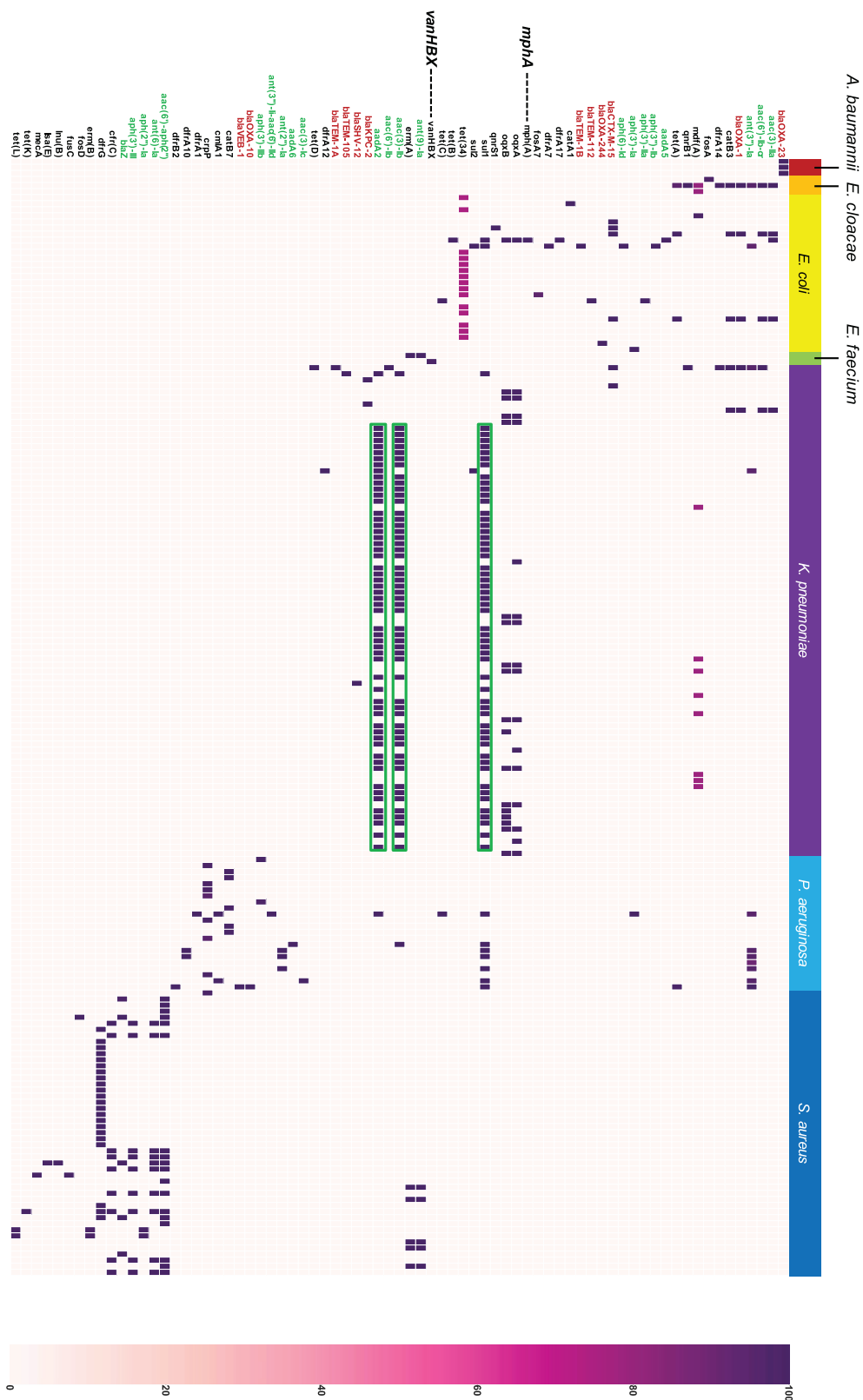


**FIG 5** Distribution of AMR genes in the prophage region. We investigated the AMR genes in prophage regions extracted from PHASTER. AMR genes were detected using the ResFinder database. The color density of the heatmap represents the identity (%) of each gene. Green frame indicates the AMR genes cassette array detected in the *K. pneumoniae*. AMR genes, highlighted in green and red, show resistant genes against aminoglycoside and  $\beta$ -lactam, respectively. Magnified AMR gene names represent AMR genes described in Results.

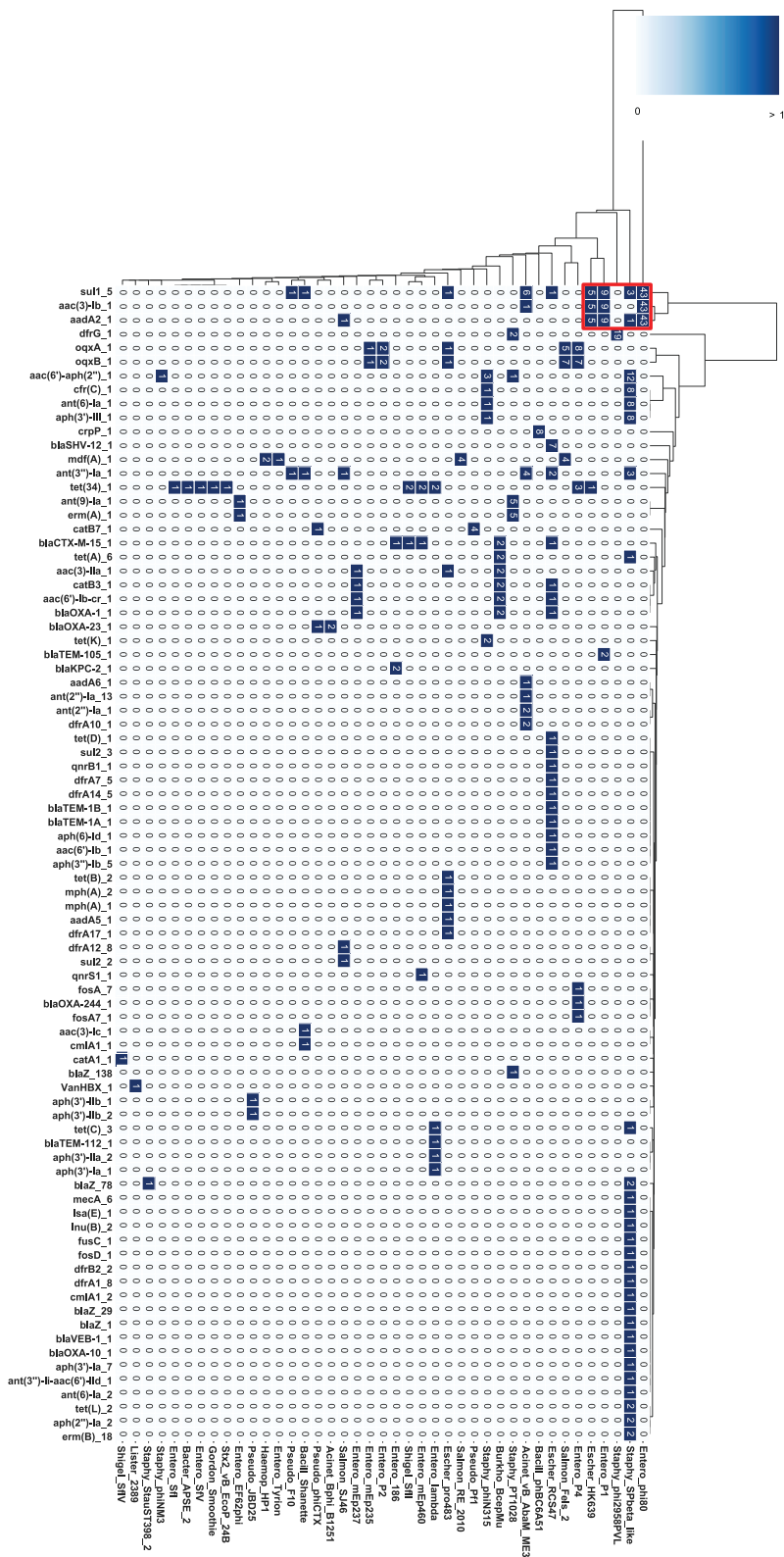


**FIG 6** Cluster analysis of AMR gene-encoding prophages. Each prophage type included in all bacterial species used in this study was clustered under the same prophage name and visualized via a heatmap. The figure was created using seaborn, which is a Python module, and cluster method, which is a hierarchical clustering method (single linkage method). The numerical characters in cells mean the number of AMR genes in the indicated prophage. The red frames indicate the examples of cassette arrays of AMR genes in the prophage region.

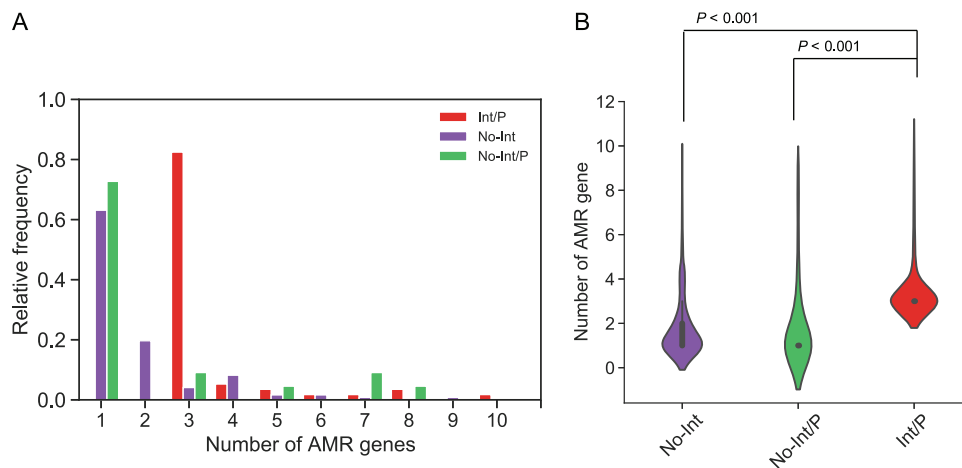


**FIG 7** Comparison of the number of AMR genes with and without an integron. No-Int is a strain that does not have an integron, No-Int/P represents that the integron is located out of the prophage region, and Int/P is a strain that has an integron in the prophage. Integron within a prophage was classified according to whether it has class 1 integrase or not. (A) A histogram shows the relative frequency of each number of AMR genes in each classification. (B) A boxplot shows the number of AMR genes in each classification. The notch of the boxplot represents the median, and Welch's *t* test was performed, with  $P < 0.05$  considered significant.

structural proteins. Although most phage-related genes in HK639 harbored by CP018816 are degraded, BLAST comparison (based on nucleotide sequences) showed that the sequences of these genes are identical to the distal sequences of other HK639 regions. This result implies that the HK639-like phages are excised from the CP018816 genome, but the end of the HK639-like phage sequence are left in the host genome. AMR genes are located at integron structures at the end of the HK639 prophage region (integron-associated prophage structures), indicating that the chromosomal locus where the prophage has integrated can accommodate other elements, such as transposons and AMR genes; this locus can be transferred to other bacteria via specialized or generalized transduction (18).

## DISCUSSION

In this study, we collected the prophage elements from a total of 1,623 complete genomes of nosocomial AMR pathogens deposited in a public database and characterized AMR and VF genes harbored. Due to multidrug resistance, ESKAPE bacteria have become a threat to global health, especially in elderly patients. HGT agents such as plasmids, prophages, and transposons often carry AMR and VF genes and move from bacteria to bacteria. Phage or prophage-carrying AMR genes are reported to be minor HGT agents (37, 38). In recent years, however, several studies have reported that AMR genes are present in the phage or prophage region (39–42), implying that they are associated with the prophage region more than expected. Nevertheless, there have been few reports comprehensively identifying and analyzing AMR/VF genes located in the prophage region of nosocomial AMR pathogens.

Our study demonstrated that the proportion of bacteria carrying AMR genes on prophage-like elements reached up to 21% (Fig. 1). Furthermore, our analysis showed that the integron-associated prophage structure is often located at the side of AMR genes (Fig. 8). Our results suggest that the number of AMR genes encoded by integron-associated prophages was higher than that of those encoded in the genome of phage particles and that AMR genes were preferentially accumulated in the prophage sequence and were stably inherited in the host genome (6). To date, plasmids are the most well-studied HGT agent. Nonetheless, we did not compare the AMR gene richness between plasmids and prophage regions. Several prophage-like elements encoding AMR genes were inserted and shared AMR genes in a plasmid; thus, we solely

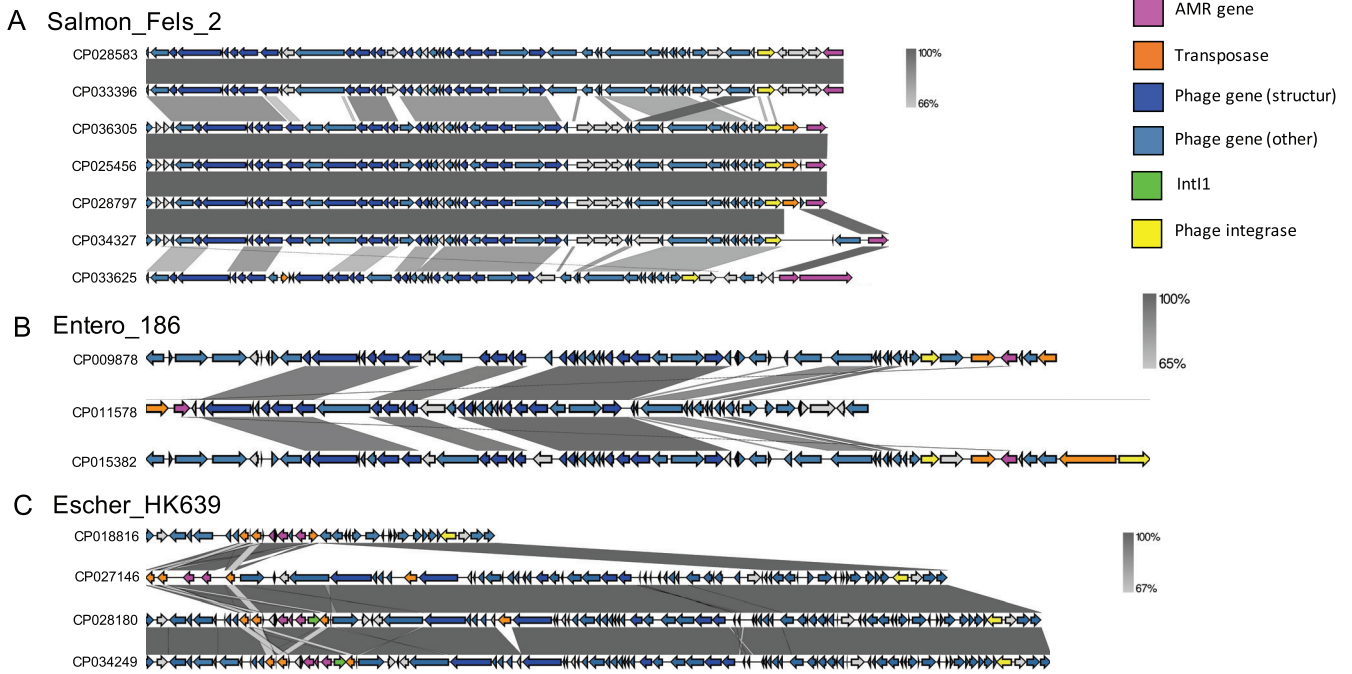


**FIG 8** Comparative analysis of sequences and positional characteristics of AMR genes located in prophages. Representative prophage type names were selected based on genome completeness. Prophage sequences were defined via the attachment sites (*attL* and *attR*). Three representative prophages—Salmon\_Fels\_2 prophage (A), Entero\_186 (B), and Escher\_HK639 (C)—were selected and visualized to show the structural feature of prophage and AMR genes. The sequences of each prophage were selected at random, and gray-shaded regions represent sequence similarity. Int1 shows the class 1 integrase, which is indicated by the green arrow, and phage-derived integrase is indicated by the yellow arrow. AMR genes are shown in magenta. Phage genes were shown by blue (structural genes) and steel blue (other than structural genes) arrow. The figures were drawn using Easyfig 2.2.2.

focused on the prevalence of AMR genes encoded by prophage regions to shed light on the previously overlooked contributions of prophages in AMR gene propagation.

Prophage induction is triggered mainly by DNA damage via SOS response, and the host is lysed by the phage lysin. We found that 46.2% of AMR gene-harboring prophages were defective, whereas intact prophages were dominant among VF gene-harboring prophages (75.2%) (Fig. 3). A previous study has shown that prophages confer antibiotic resistance to the host and result in an increase of host viability (43). In other words, the host takes the advantage of AMR gene products of prophages for survival. A recent study has reported that the induction frequency of prophage carrying AMR genes decreases under the presence of antibiotics (44). As a result, prophages tend to become defective more frequently and are inherited in the host genome (45). In contrast, it has been reported that VF genes encoded in prophage can contribute to increasing phage infectivity by increasing the burst size and the latent period (46). In addition, prophages often harbor the genes involved in superinfection exclusion, a phenomenon in which phage or prophage prevents infection by other phages (47, 48), and such genes are associated with host virulence (46). Therefore, we speculated that VF genes encoded in prophages have presumably more benefits for the prophage rather than for the bacteria, and the selective pressure of becoming defective is hardly caused in VF gene-encoding prophage. As a result, prophages containing VF genes tend to remain “intact” with phage structural genes.

Our results showed that most VF genes on prophage element were species specific (Fig. 5), presumably because the mechanism of virulence to the host, such as entry into the mammalian body (cell), and the toxicity differs depending on the species. Thus, each VF gene, which is responsible for virulence, could be detected in a species-specific manner. In contrast, modes of action of antimicrobials are common among bacterial species, and AMR genes are mobilized among bacterial genera through horizontal transfer; thus, similar AMR genes encoded in prophage elements are conserved in various bacterial species.

We found that many prophages harboring AMR genes possessed an integron structure, and the numbers of AMR genes in integron-harboring prophages were significantly higher than in prophage regions without an integron (Fig. 8). Recently, P1-like phage element sequences with integron structures have been detected in several plasmids of pathogenic *E. coli* (41) and P1-like phage group has been found at plasmids in various bacterial phyla (49). However, whether bacterial genomes harbor the integron-associated prophage structures has not yet been ascertained. Our results clearly showed that such a structure was detected in the genomes of *K. pneumoniae*, *P. aeruginosa*, and *E. coli* (Fig. 8; see also Data Set S2). Even if prophages carrying AMR genes do not possess integron structures, recombination elements, such as transposase and phage site-specific integrase genes, are located close to AMR genes (Fig. 8). Indeed, the Mu-like phage is present on a plasmid, and transposon Tn21 is encoded within the phage region of the plasmid, which also includes AMR genes (50). Although our results do not directly prove the hypothesis that AMR genes adjacent to prophages are acquired by phage transduction, prophage-related recombination genes and integrons harbored by prophages probably accommodate the AMR genes. Our analysis suggests that unlike prophages containing AMR-encoding genes, prophages containing VF-encoding genes are not likely to possess recombination-related genes near to VF genes.

It has been known that genes encoding aminoglycoside modification enzymes and  $\beta$ -lactamase are widely conserved among various species (51, 52). In this study, aminoglycoside modification enzymes and  $\beta$ -lactamase were detected in prophages and prophage-like elements of almost all genera, in accordance with previous studies (51, 52) (Fig. 5). This result suggests that phages were involved in the HGT of these highly distributed AMR genes. In fact, some AMR genes ( $\beta$ -lactamase-encoding genes) that are associated with phage-related mobile elements are widely distributed across various members of the family *Enterobacteriaceae* (53).

This study has some limitations. The sample number is uneven between each species. For example, the sample number of *E. cloacae* was 27, while that of *S. aureus* was 408. Since most of the complete genomes of *E. coli* are enterohemorrhagic *E. coli* (EHEC) genomes, Stx (classified as “toxin” in Fig. S3) and type III secretion systems were detected using the VFDB, in agreement with previous reports (54, 55). Therefore, the distribution of VF genes and the percentage of toxin and type III system harbored by prophages may have been influenced by the *E. coli* EHEC data. To analyze detailed and precise prophage sequence structure, we utilized a highly accurate prophage sequence using the National Center for Biotechnology Information (NCBI) RefSeq (56). Because most of these samples registered in RefSeq are isolated from the clinical settings or represent pathogenic bacteria, these samples may be associated with bias. Further analyses, such as metagenomic approaches, are required for more equitable assessments of the role of HGT in phages. In fact, metagenomic studies have revealed that phage fractions from various samples contain AMR genes (15, 57).

Overall, we comprehensively detected AMR and VF genes in a wide range of strains, and our results will shed light on the important roles of phages as reservoirs and factors that transfer AMR/VF genes. Further research is needed to elucidate the number of AMR and VF genes that are transferred to other strains via transduction in a clinical and natural environment.

## MATERIALS AND METHODS

**Data collection and prophage region detection.** We compiled complete genomes and RefSeq data of seven bacterial species (169 sequences of *A. baumannii*, 27 sequences of *E. cloacae*, 324 sequences of *E. coli*, 88 sequences of *E. faecium*, 408 sequences of *K. pneumoniae*, 183 sequences of *P. aeruginosa*, and 424 sequences of *S. aureus*) from GenBank using Biopython version 1.76 (58). Complete genome data sets were collected in December 2019. The genome size for each strain was referred to as the value described in GenBank (see Data Set S1). Since *E. coli* had a large number of registrations at the NCBI, GenBank accession numbers were randomly selected so that the sample size would not increase. To detect prophages and prophage-like elements (28) for each strain, we used a custom application programming interface from PHASTER (32). Prophage names were identified using the most common

phage species indicated by PHASTER. In addition, PHASTER was also used to classify prophages as either intact, questionable, or incomplete based on the length of the phage region and the number of phage-derived genes (see Data Sets S4 and S5).

**Detection of AMR and VF genes.** AMR and VF genes encoded by the prophage sequences were extracted using ABRicate version 1.0.1 (<https://github.com/tseemann/abricate>) under default settings. The ResFinder database (59) was used to detect AMR genes, and the Virulence Factors Database (VFDB) (60) was used to detect VF genes. VFs were classified based on VFDB keywords, and redundant (similar) keywords were summarized into short words (e.g., “adhesion,” “apoptosis and adherence,” and “invasive” keywords were integrated into “adherence,” and toxin-based genes were integrated into “toxin”). The same gene with a few, different mutations were distinguished as an accession number were assigned to each gene containing the respective mutation. Each of the genes was also assigned a “\_X” suffix.

**Selection of prophage regions harboring AMR and VF genes.** Prophage element regions comprising AMR/VF genes were further selected to eliminate genomic islands such as ISs and integrons without any phage-related genes. The open reading frames (ORFs) of prophage regions containing AMR and VF genes were selected using Prokka (61) with default settings; the functional annotation of ORFs were performed using local BLASTp (62). The number of prophage-related genes in each prophage region were counted. The phage-related genes did not include integron integrase, transposase, and any AMR/VF genes. If prophage regions have more than four prophage-related genes whose E value is less than 2E–20, these regions were considered true prophage regions.

**Integron analysis.** Integrons and antibiotic cassette gene arrays in prophages were detected using INTEGRALL (63). Ambiguous integrases encoded in prophage region were examined using BLASTP (protein–protein BLAST). If the amino acid identity was more than 80%, it was considered a class 1 integrase. Numbers were assigned based on the order of the gene cassette, and we referred to the number described in INTEGRALL. We classified the results into three groups, depending on the type of integron arrangement, as follows: (i) prophage region with a class 1 integrase (Int/P); (ii) prophage region without a class 1 integrase (No-Int); and (iii) integrase present but it did not exist in the prophage region (No-Int/P).

**Prophage elements and other data visualization.** Prophage elements encoding *bsh* and *clpP* were visualized using BLAST Ring Image Generator (BRIG) version 0.95 (35). All BRIG parameters were set to default. Other prophage-related regions containing AMR genes were visualized using Easyfig version 2.2.2 (64). The thresholds of BLAST hits in Easyfig were analyzed using the default value. To visualize, we selected Escher\_HK639, Entero\_186, and Salmon\_Fels\_2, which were regarded as “intact” phages, encoding a phage structure protein. Alternatively, we selected AcinetovB\_AbaM\_ME3, Entero\_phi80, and Escher\_RCS47, which were considered “incomplete” or “questionable” in PHASTER. The host accession number used for the analysis had three to five strains selected at random for each prophage. Other data were analyzed and visualized using Python 3.7.6 (Python Software Foundation, <https://www.python.org>), Matplotlib version 3.1.3, and Seaborn version 0.11.0.

**Statistical analysis.** Pearson R correlation was calculated using the default jointplot function in Seaborn. All statistical analyses were conducted using a two-sided Welch’s *t* test with Python version 3.7.6 and SciPy Module version 1.4.1, and  $P < 0.05$  was considered a significant difference.

**Data availability.** This study was performed using complete genomes registered on the NCBI. All accession numbers are listed in Data Set S1. All information on AMR and VF genes detected in this study are described in Data Sets S2 and S3. The information on integron is summarized in Data Set S2. Information on specific phage genes and the presence of attachment sites (*attL* and *attR*) in each prophage region is presented in Data Sets S4 and S5.

## SUPPLEMENTAL MATERIAL

Supplemental material is available online only.

**FIG S1**, PDF file, 0.3 MB.

**FIG S2**, PDF file, 0.4 MB.

**FIG S3**, PDF file, 0.1 MB.

**FIG S4**, PDF file, 0.2 MB.

**DATA SET S1**, XLSX file, 0.1 MB.

**DATA SET S2**, XLSX file, 0.03 MB.

**DATA SET S3**, XLSX file, 0.03 MB.

**DATA SET S4**, XLSX file, 0.02 MB.

**DATA SET S5**, XLSX file, 0.02 MB.

## ACKNOWLEDGMENTS

We are grateful to Yoshitoshi Ogura for his valuable suggestions on the manuscript.

This study was supported by JSPS KAKENHI (grant JP18K08455), a Grant-in-Aid for Scientific Research (C), and research activity grants from the Wesco Scientific Promotion Foundation (M.K.). This work was also supported by the Research Program on Emerging

and Re-emerging Infectious Diseases from the Japan Agency for Medical Research and Development (grants 20fk0108132j0001 and 21fk0108604j0001).

## REFERENCES

- Rice LB. 2008. Federal funding for the study of antimicrobial resistance in nosocomial pathogens: no ESKAPE. *J Infect Dis* 197:1079–1081. <https://doi.org/10.1086/533452>.
- Mulani MS, Kamble EE, Kumkar SN, Tawre MS, Pardesi KR. 2019. Emerging strategies to combat ESKAPE pathogens in the era of antimicrobial resistance: a review. *Front Microbiol* 10:539. <https://doi.org/10.3389/fmicb.2019.00539>.
- Chong Y, Shimoda S, Shimono N. 2018. Current epidemiology, genetic evolution, and clinical impact of extended-spectrum  $\beta$ -lactamase-producing *Escherichia coli* and *Klebsiella pneumoniae*. *Infect Genet Evol* 61:185–188. <https://doi.org/10.1016/j.meegid.2018.04.005>.
- Choi J, Kotay SM, Goel R. 2010. Various physico-chemical stress factors cause prophage induction in *Nitrosospora multififormis* 25196, an ammonia-oxidizing bacterium. *Water Res* 44:4550–4558. <https://doi.org/10.1016/j.watres.2010.04.040>.
- Boling L, Cuevas DA, Grasis JA, Kang HS, Knowles B, Levi K, Maughan H, McNair K, Rojas MI, Sanchez SE, Smurthwaite C, Rohwer F. 2020. Dietary prophage inducers and antimicrobials: toward landscaping the human gut microbiome. *Gut Microbes* 11:721–734. <https://doi.org/10.1080/19490976.2019.1701353>.
- Bobay LM, Rocha EPC, Touchon M. 2013. The adaptation of temperate bacteriophages to their host genomes. *Mol Biol Evol* 30:737–751. <https://doi.org/10.1093/molbev/mss279>.
- Croucher NJ, Coupland PG, Stevenson AE, Callendrello A, Bentley SD, Hanage WP. 2014. Diversification of bacterial genome content through distinct mechanisms over different timescales. *Nat Commun* 5:5471. <https://doi.org/10.1038/ncomms6471>.
- Wyres KL, Wick RR, Judd LM, Froumine R, Tokolyi A, Gorrie CL, Lam MMC, Duchêne S, Jenney A, Holt KE. 2019. Distinct evolutionary dynamics of horizontal gene transfer in drug-resistant and virulent clones of *Klebsiella pneumoniae*. *PLoS Genet* 15:e1008114. <https://doi.org/10.1371/journal.pgen.1008114>.
- Shen J, Zhou J, Xu Y, Xiu Z. 2020. Prophages contribute to genome plasticity of *Klebsiella pneumoniae* and may involve the chromosomal integration of ARGs in CG258. *Genomics* 112:998–1010. <https://doi.org/10.1016/j.ygeno.2019.06.016>.
- de Sousa JAM, Buffet A, Haudiquet M, Rocha EPC, Rendueles O. 2020. Modular prophage interactions driven by capsule serotype select for capsule loss under phage predation. *ISME J* 14:2980–2987. <https://doi.org/10.1038/s41396-020-0726-z>.
- Silver-Mysliwiec TH, Bramucci MG. 1990. Bacteriophage-enhanced sporulation: comparison of spore-converting bacteriophages PMB12 and SP10. *J Bacteriol* 172:1948–1953. <https://doi.org/10.1128/jb.172.4.1948-1953.1990>.
- McGrath S, Fitzgerald GF, Van Sinderen D. 2002. Identification and characterization of phage-resistance genes in temperate lactococcal bacteriophages. *Mol Microbiol* 43:509–520. <https://doi.org/10.1046/j.1365-2958.2002.02763.x>.
- Aucouturier A, Chain F, Langella P, Bidnenko E. 2018. Characterization of a prophage-free derivative strain of *Lactococcus lactis* ssp. *lactis* IL1403 reveals the importance of prophages for phenotypic plasticity of the host. *Front Microbiol* 9:2032. <https://doi.org/10.3389/fmicb.2018.02032>.
- Brown-Jaque M, Calero-Cáceres W, Muniesa M. 2015. Transfer of antibiotic-resistance genes via phage-related mobile elements. *Plasmid* 79:1–7. <https://doi.org/10.1016/j.plasmid.2015.01.001>.
- Gómez-Gómez C, Blanco-Picazo P, Brown-Jaque M, Quirós P, Rodríguez-Rubio L, Cerdà-Cuellar M, Muniesa M. 2019. Infectious phage particles packaging antibiotic resistance genes found in meat products and chicken feces. *Sci Rep* 9:13281. <https://doi.org/10.1038/s41598-019-49898-0>.
- López-Leal G, Santamaria RI, Cevallos MÁ, Gonzalez V, Castillo-Ramírez S. 2020. Prophages encode antibiotic resistance genes in *Acinetobacter baumannii*. *Microb Drug Resist* 26:1275–1277. (Letter). <https://doi.org/10.1089/mdr.2019.0362>.
- Anand T, Bera BC, Vaid RK, Barua S, Riyesh T, Virmani N, Hussain M, Singh RK, Tripathi BN. 2016. Abundance of antibiotic resistance genes in environmental bacteriophages. *J Gen Virol* 97:3458–3466. <https://doi.org/10.1099/jgv.0.000639>.
- Rands CM, Starikova EV, Brüssow H, Kriventseva EV, Govorun VM, Zdobnov EM. 2018. ACI-1 beta-lactamase is widespread across human gut microbiomes due to transposons harboured by tailed prophages. *Environ Microbiol* 20:2288–2300. <https://doi.org/10.1111/1462-2920.14276>.
- Moon K, Jeon JH, Kang I, Park KS, Lee K, Cha CJ, Lee SH, Cho JC. 2020. Freshwater viral metagenome reveals novel and functional phage-borne antibiotic resistance genes. *Microbiome* 8:75. <https://doi.org/10.1186/s40168-020-00863-4>.
- Brown-Jaque M, Oyarzun LR, Cornejo-Sánchez T, Martín-Gómez MT, Gartner S, de Gracia J, Rovira S, Alvarez A, Jofre J, González-López JJ, Muniesa M. 2018. Detection of bacteriophage particles containing antibiotic resistance genes in the sputum of cystic fibrosis patients. *Front Microbiol* 9:856. <https://doi.org/10.3389/fmicb.2018.00856>.
- Costa AR, Monteiro R, Azeredo J. 2018. Genomic analysis of *Acinetobacter baumannii* prophages reveals remarkable diversity and suggests profound impact on bacterial virulence and fitness. *Sci Rep* 8:15346. <https://doi.org/10.1038/s41598-018-33800-5>.
- Bae T, Baba T, Hiramatsu K, Schneewind O. 2006. Prophages of *Staphylococcus aureus* Newman and their contribution to virulence. *Mol Microbiol* 62:1035–1047. <https://doi.org/10.1111/j.1365-2958.2006.05441.x>.
- Dini M, Shokohizadeh L, Jalilian FA, Moradi A, Arabestani MR. 2019. Genotyping and characterization of prophage patterns in clinical isolates of *Staphylococcus aureus*. *BMC Res Notes* 12:669. <https://doi.org/10.1186/s13104-019-4711-4>.
- Hayashi T, Makino K, Ohnishi M, Kurokawa K, Ishii K, Yokoyama K, Han CG, Ohtsubo E, Nakayama K, Murata T, Tanaka M, Tobe T, Iida T, Takami H, Honda T, Sasakawa C, Ogasawara N, Yasunaga T, Kuhara S, Shiba T, Hattori M, Shinagawa H. 2001. Complete genome sequence of enterohemorrhagic *Escherichia coli* O157:H7 and genomic comparison with a laboratory strain K-12. *DNA Res* 8:11–22. <https://doi.org/10.1093/dnares/8.1.11>.
- Zhang Y, Te Liao Y, Salvador A, Sun X, Wu VCH. 2019. Prediction, diversity, and comparative analysis of temperate phages induced from Shiga toxin-producing *Escherichia coli* strains. *Front Microbiol* 10:3093. <https://doi.org/10.3389/fmicb.2019.03093>.
- Cooke FJ, Wain J, Fookes M, Ivens A, Thomson N, Brown DJ, Threlfall EJ, Gunn G, Foster G, Dougan G. 2007. Prophage sequences defining hot spots of genome variation in *Salmonella enterica* serovar Typhimurium can be used to discriminate between field isolates. *J Clin Microbiol* 45:2590–2598. <https://doi.org/10.1128/JCM.00729-07>.
- Waldor MK, Mekalanos JJ. 1996. Lysogenic conversion by a filamentous phage encoding cholera toxin. *Science* 272:1910–1913. <https://doi.org/10.1126/science.272.5270.1910>.
- Castillo D, Kauffman K, Hussain F, Kalatzis P, Rørbo N, Polz MF, Middelboe M. 2018. Widespread distribution of prophage-encoded virulence factors in marine *Vibrio* communities. *Sci Rep* 8:9973. <https://doi.org/10.1038/s41598-018-28326-9>.
- Kimmit PT, Harwood CR, Barer MR. 1999. Induction of type 2 Shiga toxin synthesis in *Escherichia coli* O157 by 4-quinolones. *Lancet* 353:1588–1589. [https://doi.org/10.1016/S0140-6736\(99\)00621-2](https://doi.org/10.1016/S0140-6736(99)00621-2).
- Goerke C, Koller J, Wolz C. 2006. Ciprofloxacin and trimethoprim cause phage induction and virulence modulation in *Staphylococcus aureus*. *Antimicrob Agents Chemother* 50:171–177. <https://doi.org/10.1128/AAC.50.1.171-177.2006>.
- Rezaei Javan R, Ramos-Sevillano E, Akter A, Brown J, Brueggemann AB. 2019. Prophages and satellite prophages are widespread in *Streptococcus* and may play a role in pneumococcal pathogenesis. *Nat Commun* 10:4852. <https://doi.org/10.1038/s41467-019-12825-y>.
- Arndt D, Grant JR, Marcu A, Sajed T, Pon A, Liang Y, Wishart DS. 2016. PHASTER: a better, faster version of the PHAST phage search tool. *Nucleic Acids Res* 44:W16–W21. <https://doi.org/10.1093/nar/gkw387>.
- Billard-Pomares T, Foueteau S, Jacquet ME, Roche D, Barbe V, Castellanos M, Bouet JY, Cruveiller S, Médigue C, Blanco J, Clermont O, Denamur E, Branger C. 2014. Characterization of a P1-like bacteriophage carrying an SHV-2 extended-spectrum  $\beta$ -lactamase from an *Escherichia coli* strain. *Antimicrob Agents Chemother* 58:6550–6557. <https://doi.org/10.1128/AAC.03183-14>.
- Li Y, Huang J, Wang X, Xu C, Han T, Guo X. 2020. Genetic characterization of the O-antigen and development of a molecular serotyping scheme for *Enterobacter cloacae*. *Front Microbiol* 11:727. <https://doi.org/10.3389/fmicb.2020.00727>.

35. Alikhan NF, Petty NK, Ben Zakour NL, Beatson SA. 2011. BLAST Ring Image Generator (BRIG): simple prokaryote genome comparisons. *BMC Genomics* 12:402. <https://doi.org/10.1186/1471-2164-12-402>.
36. Dussurget O, Cabanes D, Dehoux P, Lecuit M, Buchrieser C, Glaser P, Cossart P, European Listeria Genome Consortium. 2002. *Listeria monocytogenes* bile salt hydrolase is a PrfA-regulated virulence factor involved in the intestinal and hepatic phases of listeriosis. *Mol Microbiol* 45:1095–1106. <https://doi.org/10.1046/j.1365-2958.2002.03080.x>.
37. Enault F, Briet A, Bouteille L, Roux S, Sullivan MB, Petit MA. 2017. Phages rarely encode antibiotic resistance genes: a cautionary tale for virome analyses. *ISME J* 11:237–247. <https://doi.org/10.1038/ismej.2016.90>.
38. Volkova VV, Lu Z, Besser T, Gröhn YT. 2014. Modeling the infection dynamics of bacteriophages in enteric *Escherichia coli*: estimating the contribution of transduction to antimicrobial gene spread. *Appl Environ Microbiol* 80:4350–4362. <https://doi.org/10.1128/AEM.00446-14>.
39. Modi SR, Lee HH, Spina CS, Collins JJ. 2013. Antibiotic treatment expands the resistance reservoir and ecological network of the phage metagenome. *Nature* 499:219–222. <https://doi.org/10.1038/nature12212>.
40. Colomer-Lluch M, Calero-Cáceres W, Jebri S, Hmaied F, Muniesa M, Jofre J. 2014. Antibiotic resistance genes in bacterial and bacteriophage fractions of Tunisian and Spanish wastewaters as markers to compare the antibiotic resistance patterns in each population. *Environ Int* 73:167–175. <https://doi.org/10.1016/j.envint.2014.07.003>.
41. Venturini C, Zingali T, Wyrsh ER, Bowring B, Iredell J, Partridge SR, Djordjevic SP. 2019. Diversity of P1 phage-like elements in multidrug-resistant *Escherichia coli*. *Sci Rep* 9:18861. <https://doi.org/10.1038/s41598-019-54895-4>.
42. Wang M, Zeng Z, Jiang F, Zheng Y, Shen H, Macedo N, Sun Y, Sahin O, Li G. 2020. Role of enterotoxigenic *Escherichia coli* prophage in spreading antibiotic resistance in a porcine-derived environment. *Environ Microbiol* 22:4974–4984. <https://doi.org/10.1111/1462-2920.15084>.
43. Wang X, Kim Y, Ma Q, Hong SH, Pokusaeva K, Sturino JM, Wood TK. 2010. Cryptic prophages help bacteria cope with adverse environments. *Nat Commun* 1:147. <https://doi.org/10.1038/ncomms1146>.
44. Wendling C, Refardt D, Hall A. 2020. Fitness benefits to bacteria of carrying prophages and prophage-encoded antibiotic-resistance genes peak in different environments. *bioRxiv* <https://doi.org/10.1101/2020.03.13.990044>.
45. Bobay LM, Touchon M, Rocha EPC. 2014. Pervasive domestication of defective prophages by bacteria. *Proc Natl Acad Sci U S A* 111:12127–12132. <https://doi.org/10.1073/pnas.1405336111>.
46. Abedon ST, LeJeune JT. 2005. Why bacteriophage encode exotoxins and other virulence factors. *Evol Bioinform Online* 1:117693430500100–117693430500110. <https://doi.org/10.1177/1176934305001000001>.
47. Bondy-Denomy J, Qian J, Westra ER, Buckling A, Guttman DS, Davidson AR, Maxwell KL. 2016. Prophages mediate defense against phage infection through diverse mechanisms. *ISME J* 10:2854–2866. <https://doi.org/10.1038/ismej.2016.79>.
48. Dedrick RM, Jacobs-Sera D, Guerrero Bustamante CA, Garlena RA, Mavrich TN, Pope WH, Cervantes Reyes JC, Russell DA, Adair T, Alvey R, Bonilla JA, Bricker JS, Brown BR, Byrnes D, Cresawn SG, Davis WB, Dickson LA, Edgington NP, Findley AM, Golebiewska U, Grose JH, Hayes CF, Hughes LE, Hutchison KW, Isern S, Johnson AA, Kenna MA, Klyczek KK, Magee CM, Michael SF, Molloy SD, Montgomery MT, Neitzel J, Page ST, Pizzorno MC, Poxleitner MK, Rinehart CA, Robinson CJ, Rubin MR, Teyim JN, Vazquez E, Ware VC, Washington J, Hatfull GF. 2017. Prophage-mediated defence against viral attack and viral counter-defence. *Nat Microbiol* 2:16251. <https://doi.org/10.1038/nmicrobiol.2016.251>.
49. Pfeifer E, Moura de Sousa JA, Touchon M, Rocha EPC. 2021. Bacteria have numerous distinctive groups of phage–plasmids with conserved phage and variable plasmid gene repertoires. *Nucleic Acids Res* 49:2655–2673. <https://doi.org/10.1093/nar/gkab064>.
50. Radstrom P, Skold O, Swedberg G, Flensburg J, Roy PH, Sundstrom L. 1994. Transposon Tn5090 of plasmid R751, which carries an integron, is related to Tn7, Mu, and the retroelements. *J Bacteriol* 176:3257–3268. <https://doi.org/10.1128/jb.176.11.3257-3268.1994>.
51. Fouhy F, Ogilvie LA, Jones BV, Ross RP, Ryan AC, Dempsey EM, Fitzgerald GF, Stanton C, Cotter PD. 2014. Identification of aminoglycoside and  $\beta$ -lactam resistance genes from within an infant gut functional metagenomic library. *PLoS One* 9:e108016. <https://doi.org/10.1371/journal.pone.0108016>.
52. Ullmann IF, Tunsjø HS, Andreassen M, Nielsen KM, Lund V, Charnock C. 2019. Detection of aminoglycoside-resistant bacteria in sludge samples from Norwegian drinking water treatment plants. *Front Microbiol* 10:487. <https://doi.org/10.3389/fmicb.2019.00487>.
53. Oliver A, Coque TM, Alonso D, Valverde A, Baquero F, Cantón R. 2005. CTX-M-10 linked to a phage-related element is widely disseminated among *Enterobacteriaceae* in a Spanish Hospital. *Antimicrob Agents Chemother* 49:1567–1571. <https://doi.org/10.1128/AAC.49.4.1567-1571.2005>.
54. Melton-Celsa AR. 2014. Shiga toxin (Stx) classification, structure, and function. *Microbiol Spectr* 2:EHEC-0024–0013. <https://doi.org/10.1128/microbiolspec.EHEC-0024-2013>.
55. Jarvis KG, Girón JA, Jerse AE, McDaniel TK, Donnenberg MS, Kaper JB. 1995. Enteropathogenic *Escherichia coli* contains a putative type III secretion system necessary for the export of proteins involved in attaching and effacing lesion formation. *Proc Natl Acad Sci U S A* 92:7996–8000. <https://doi.org/10.1073/pnas.92.17.7996>.
56. d’Humières C, Touchon M, Dion S, Cury J, Ghazlane A, Garcia-Garcera M, Bouchier C, Ma L, Denamur E, P C Rocha E. 2019. A simple, reproducible, and cost-effective procedure to analyse gut phageome: from phage isolation to bioinformatic approach. *Sci Rep* 9:11331. <https://doi.org/10.1038/s41598-019-47656-w>.
57. Larrañaga O, Brown-Jaque M, Quirós P, Gómez-Gómez C, Blanch AR, Rodríguez-Rubio L, Muniesa M. 2018. Phage particles harboring antibiotic resistance genes in fresh-cut vegetables and agricultural soil. *Environ Int* 115:133–141. <https://doi.org/10.1016/j.envint.2018.03.019>.
58. Cock PJA, Antao T, Chang JT, Chapman BA, Cox CJ, Dalke A, Friedberg I, Hamelryck T, Kauff F, Wilczynski B, De Hoon MJL. 2009. Biopython: freely available Python tools for computational molecular biology and bioinformatics. *Bioinformatics* 25:1422–1423. <https://doi.org/10.1093/bioinformatics/btp163>.
59. Zankari E, Hasman H, Cosentino S, Vestergaard M, Rasmussen S, Lund O, Aarestrup FM, Larsen MV. 2012. Identification of acquired antimicrobial resistance genes. *J Antimicrob Chemother* 67:2640–2644. <https://doi.org/10.1093/jac/dks261>.
60. Chen L, Zheng D, Liu B, Yang J, Jin Q. 2016. VFDB 2016: hierarchical and refined dataset for big data analysis—10 years on. *Nucleic Acids Res* 44:D694–D697. <https://doi.org/10.1093/nar/gkv1239>.
61. Seemann T. 2014. Prokka: rapid prokaryotic genome annotation. *Bioinformatics* 30:2068–2069. <https://doi.org/10.1093/bioinformatics/btu153>.
62. Altschul SF, Gish W, Miller W, Myers EW, Lipman DJ. 1990. Basic local alignment search tool. *J Mol Biol* 215:403–410. [https://doi.org/10.1016/S0022-2836\(05\)80360-2](https://doi.org/10.1016/S0022-2836(05)80360-2).
63. Moura A, Soares M, Pereira C, Leitão N, Henriques I, Correia A. 2009. INTEGRALL: a database and search engine for integrons, integrases and gene cassettes. *Bioinformatics* 25:1096–1098. <https://doi.org/10.1093/bioinformatics/btp105>.
64. Sullivan MJ, Petty NK, Beatson SA. 2011. Easyfig: a genome comparison visualizer. *Bioinformatics* 27:1009–1010. <https://doi.org/10.1093/bioinformatics/btr039>.